Modern Valence-Bond Description of Chemical Reaction Mechanisms: The 1,3-Dipolar Addition of Diazomethane to Ethene

Joshua J. Blavins[†] and Peter B. Karadakov*,[†]

Department of Chemistry, University of Surrey, Guildford, Surrey GU2 7XH, U.K.

David L. Cooper

Department of Chemistry, University of Liverpool, P.O. Box 147, Liverpool L69 7ZD, U.K.

pbk1@york.ac.uk

The electronic mechanism for the gas-phase concerted 1,3-dipolar cycloaddition of diazomethane (CH_2N_2) to ethene (C_2H_4) is described through spin-coupled (SC) calculations at a sequence of geometries along the intrinsic reaction coordinate obtained at the MP2/6-31G(d) level of theory. It is shown that the bonding rearrangements occurring during the course of this reaction follow a heterolytic pattern, characterized by the movement of three well-identifiable orbital pairs, which are initially responsible for the π bond in ethene and the C−N π bond and one of the N−N π bonds in diazomethane and are retained throughout the entire reaction path from reactants to product. Taken together with our previous SC study of the electronic mechanism of the 1,3-dipolar cycloaddition of fulminic acid (HCNO) to ethyne (C_2H_2) (*Theor. Chim. Acc.* **1998**, *100*, 222), the results of the present work suggest strongly that most gas-phase concerted 1,3-dipolar cycloaddition reactions can be expected to follow a heterolytic mechanism of this type, which does not involve an aromatic transition state. The more conventional aspects of the gas-phase concerted 1,3-dipolar cycloaddition of diazomethane to ethene, including optimized transition structure geometry, electronic activation energy, activation barrier corrected for zero-point energies, standard enthalpy, entropy and Gibbs free energy of activation, have been calculated at the HF/6-31G(d), B3LYP/6-31G(d), MP2/6-31G(d), MP2/6-31G(d,p), QCISD/6-31G(d) and CCD/6-31G(d) levels of theory. We also report the CCD/6-311++G(2d, 2p)//CCD/6-31G(d), MP4(SDTQ)/6-311++G(2d,2p)//CCD/6-31G-(d) and CCSD(T)/6-311++G(2d, 2p)//CCD/6-31G(d) electronic activation energies.

Introduction

The two main aspects of a chemical reaction mechanism are the changes in the geometry and energy of the reacting system on the way from reactants to products and the parallel reorganization of its electronic structure, which usually involves bond-breaking and bond-making processes. The first of these can be studied using a wide range of correlated post-Hartree−Fock quantum-chemical approaches, the most advanced of which are already capable of providing conclusive results for reactions between relatively small molecules. However, with the increase of the complexity of the underlying wave functions, it becomes very difficult, if not impossible, to elucidate the qualitative features of the second aspect, the electronic structure changes throughout the reaction.

It was shown recently that a form of modern valence-bond (VB) theory, the spin-coupled (SC) approach (reviews and further references are provided within refs 1 and 2) furnishes easy-to-interpret models for the electronic mechanisms of six-electron pericyclic reactions including the Diels−Alder reaction between butadiene and ethene,[3] the 1,3-dipolar cycloaddition between fulminic acid and ethyne[4] and the electrocyclization of hexatriene[5] and, at the same time, recovers most (as a rule, more than 90%) of the nondynamical correlation energy within the six-orbital active space required for the description of the corresponding reaction pathways. In each case the SC approach produces a very clear picture of the electronic rearrangements taking place as the system approaches the transition structure (TS), at the TS itself and as the system evolves beyond the TS. It is even possible to monitor directly the progress of the bonds being broken or formed during the reaction. During the Diels−Alder reaction and the electrocyclization of hexatriene, bonds break and reform in a homolytic way; the major recoupling of the spins of the active orbitals takes place at the TS and involves a resonance pattern very similar to that in benzene. This strongly suggests that these reactions pass through an aromatic TS. An entirely different description emerges for the 1,3-dipolar cycloaddition between fulminic acid and ethyne. The bond breaking and formation now involve shifts of whole

[†] Address from May 1, 2001: Department of Chemistry, University of York, York, YO10 5DD, U.K.

(1) Gerratt, J.; Cooper, D. L.; Karadakov, P. B.; Raimondi, M. *Chem. Soc. Rev.* **1997**, *26*, 87.

(2) Gerratt, J.; Cooper, D. L.; Karadakov, P. B.; Raimondi, M. In *The Encyclopedia of Computational Chemistry*; Schleyer, P. v. R., Ed.; Wiley: New York, 1998; p 2672.

(3) Karadakov, P. B.; Cooper, D. L.; Gerratt, J. *J. Am. Chem. Soc.* **1998**, *120*, 3975.

(4) Karadakov, P. B.; Cooper, D. L.; Gerratt, J. *Theor. Chem. Acc.* **1998**, *100*, 222.

(5) Karadakov, P. B.; Cooper, D. L.; Thorsteinsson, T.; Gerratt, J. In *Quantum Systems in Chemistry and Physics. Volume 1: Basic Problems and Model Systems*; Hernández-Laguna, A., Maruani, J., McWeeny, R., Wilson, S., Eds.; Kluwer: Dordrecht, 2000; p 327.

10.1021/jo015560a CCC: $20.00
Published on Web 05/18/2001

orbital pairs rather than spin recouplings. This indicates a heterolytic mechanism and a nonaromatic TS. This description is a highly unusual outcome of the application of a VB-style approach. It requires one of the orbitals making up the electron pair to detach itself, during the course of the reaction, from the atomic center with which it is associated initially and to end up localized about another center. Classical VB theory uses strictly localized orbitals attached to particular atomic centers and is rather unlikely to predict an electronic reaction mechanism of this type. However, the shifts of whole electron pairs are possible within a description based on the SC wave function, as it makes use of singly occupied nonorthogonal orbitals that are constructed just as in standard molecular orbital (MO) theory, without any a priori assumptions about their shapes.

Of course, the analysis of the electronic mechanism of just one specific 1,3-dipolar cycloaddition does not provide sufficient ground for making more general conclusions about the nature of the electronic rearrangements that take place during typical reactions of this type. It is also not possible to exclude the possibility that the electronic mechanism of the reaction between fulminic acid and ethyne might be influenced by a particular feature of the electronic structure of the 1,3-dipole. As has been shown in previous SC work,[6] the "hypercoordinate" central nitrogen in HCNO participates in more than four covalent bonds. However, the N−O π bond is strongly polarized toward the oxygen atom (as indicated by the N to O arrow in scheme A below), which suggests that it could be facile during the cycloaddition of HCNO to ethyne for the two orbitals responsible for this bond to relocate in order to form one of the bonds closing the isoxazole ring.

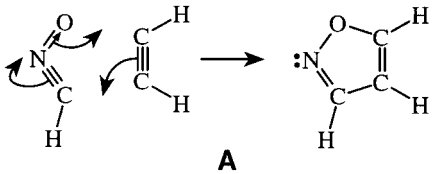

A

An electronic structure reorganization of this type could be perceived as more unlikely in reactions involving other 1,3-dipoles, such as diazomethane (CH_2N_2), in which the net polarization of the N−N π bond toward the terminal nitrogen is small (see ref 6).

The main aim of this paper is to make a significant step toward providing an answer to the question whether the electronic mechanism revealed by the previous SC study of the 1,3-dipolar cycloaddition between fulminic acid and ethyne represents an exception motivated by the particular choice of the reactants or highlights characteristic features of the electronic structure rearrangements that take place during 1,3-dipolar cycloadditions in general. We describe the SC model for the electronic mechanism of the gas-phase 1,3-dipolar cycloaddition of diazomethane to ethene, and we show that it is very closely related to that for the analogous reaction involving fulminic acid and ethyne. Additionally, the current work provides an extensive comparison and analysis of the results of a number of different quantum-chemical approaches for the more conventional aspects of this reaction, including TS geometry, electronic activation energy, activation barrier corrected for zero-point energies, standard enthalpy, entropy and Gibbs free energy of activation.

Computational Procedure

The results of a number of computational studies of cycloadditions involving unsubstituted 1,3-dipoles and dipolarophiles (see, e.g., refs 4 and 7−9) indicate that these reactions follow concerted pathways along large sections of which the reacting system retains a plane of symmetry coincident with the heavy atoms. The fact that within the SC model for the 1,3-dipolar cycloaddition of fulminic acid to ethyne[4] the orbitals participating in the processes of bond-breaking and bond-formation move in pairs (see scheme A in the Introduction) suggests that the corresponding reaction path can be described reasonably well by wave functions based on a closed-shell reference. We assumed this also to be true in the case of the 1,3-dipolar cycloaddition of diazomethane to ethene (as will be shown in the next section, this assumption is fully vindicated by the SC model for the reaction mechanism). The C_s-symmetry concerted transition structure (TS) for this reaction, as well as the geometries of the reactants, diazomethane and ethene, and of the product, 1-pyrazoline, were optimized using Hartree−Fock [HF/6-31G(d)], density functional theory [B3LYP/6-31G(d)], Møller−Plesset perturbation theory [MP2/6-31G(d) and MP2/6-31G(d,p)], quadratic configuration-interaction [QCISD/6-31G(d)] and coupled-cluster [CCD/6-31G(d)] approaches. Additionally, single-point energies for CCD/6-311++G(2d,2p), MP4(SDTQ)/6-311++G(2d,2p) and CCSD(T)/6-311++G(2d,2p) wave functions were evaluated at the CCD/6-31G(d) TS, reactant and product geometries. The intrinsic reaction coordinate (IRC) was calculated at the MP2/6-31G(d) level of theory, starting from the corresponding TS, in steps of about 0.1 amu$^{1/2}$bohr, until local minima were reached both in the direction of the reactants and in the direction of the product. All geometry optimizations and the IRC calculation were performed using GAUSSIAN98[10] and satisfy the default convergence criteria. The MP*n*, QCISD and CC wave functions used in this paper incorporate the default "frozen-core" (FC) approximation. All optimized TS geometries were shown to be first-order saddle points on the corresponding energy hypersurfaces through diagonalization of the analytic (for HF, B3LYP and MP2 wave functions) or numerical (for QCISD and CCD wave functions) Hessians calculated at these geometries.

It is generally accepted that 1,3-dipolar cycloaddition reactions involve four π electrons from the 1,3-dipole and two from the dipolarophile. The description of the electronic mechanism of a reaction of this type requires the use of a SC wave function with not less than six active (or, spin-coupled) orbitals. In the case of the 1,3-dipolar cycloaddition of diazomethane to ethene the appropriate SC(6) wave function can be written as

$$\Psi_{00}^{6} = \hat{A}[(\prod_{i=1}^{16}\varphi_i\alpha\varphi_i\beta)(\prod_{\mu=1}^{6}\psi_\mu)\Theta_{00}^{6}] \qquad (1)$$

(6) Cooper, D. L.; Gerratt, J.; Raimondi, M.; Wright, S. C. *J. Chem. Soc., Perkin Trans. 2* **1989**, 1187.

(7) McDouall, J. J. W.; Robb, M. A.; Niazi, U.; Bernardi, F.; Schlegel, H. B. *J. Am. Chem. Soc.* **1987**, *109*, 4642.

(8) Rastelli, A.; Gandolfi, R.; Amadé, M. S. *J. Org. Chem.* **1998**, *63*, 7425.

(9) M. T. Nguyen, A. K.; Chandra, S. S.; Morokuma, K. *J. Org. Chem.* **1999**, *64*, 65.

(10) Frisch, M. J.; Trucks, G. W.; Schlegel, H. B.; Scuseria, G. E.; Robb, M. A.; Cheeseman, J. R.; Zakrzewski, V. G.; J. A. Montgomery, J.; Stratmann, R. E.; Burant, J. C.; Dapprich, S.; Millam, J. M.; Daniels, A. D.; Kudin, K. N.; Strain, M. C.; Farkas, O.; Tomasi, J.; Barone, V.; Cossi, M.; Cammi, R.; Mennucci, B.; Pomelli, C.; Adamo, C.; Clifford, S.; Ochterski, J.; Petersson, G. A.; Ayala, P. Y.; Cui, Q.; Morokuma, K.; Malick, D. K.; Rabuck, A. D.; Raghavachari, K.; Foresman, J. B.; Cioslowski, J.; Ortiz, J. V.; Baboul, A. G.; Stefanov, B. B.; Liu, G.; Liashenko, A.; Piskorz, P.; Komaromi, I.; Gomperts, R.; Martin, R. L.; Fox, D. J.; Keith, T.; Al-Laham, M. A.; Peng, C. Y.; Nanayakkara, A.; Gonzalez, C.; Challacombe, M.; Gill, P. M. W.; Johnson, B.; Chen, W.; Wong, M. W.; Andres, J. L.; Head-Gordon, M.; Replogle, E. S.; Pople, J. A. *Gaussian 98, Revision A.7*; Gaussian, Inc.: Pittsburgh, PA, 1998.

The only difference between this wave function and the one used to describe the reaction between fulminic acid and ethyne[4] is in the number of doubly occupied (or, inactive) orbitals (φ_i), which has increased by one in order to accommodate the larger number of core electrons. By definition, the six SC orbitals (ψ_μ) are singly occupied and nonorthogonal; all active and inactive orbitals are approximated, as in most MO-type approaches, by linear expansions in a suitable basis of atomic orbitals (AOs) contributed by all atoms in the system. The active-space spin function (eq 2) is constructed as a most

$$\Theta^6_{00} = \sum_{k=1}^{5} C_{0k}\Theta^6_{00;k} \tag{2}$$

general linear combination of all five unique spin coupling schemes $\Theta^6_{00;k}$ for a singlet system of six electrons. The zero values of the total spin S and its z-projection M are reflected in the zero subscripts attached to Θ^6_{00}, C_{0k} and $\Theta^6_{00;k}$. (The spin-coupling coefficients C_{0k} depend on S only and thus require a single subscript, while Θ^6_{00} and $\Theta^6_{00;k}$ depend on both S and M.)

All orbital and spin-coupling coefficients that enter the SC wave function were determined variationally, by optimizing the corresponding energy expectation value. SC calculations were carried out at the MP2/6-31G(d) TS geometry of the reacting system and at selected points along the corresponding IRC using the methodology described in ref 11. All one- and two-electron integrals (6-31G basis) required by the SC code were evaluated using the GAMESS-US program package.[12]

To highlight different features of the overall active-space spin-coupling pattern Θ^6_{00} (see eq 2), SC theory often uses different sets of spin eigenfunctions $\Theta^6_{00;k}$, particularly those introduced by Kotani, Rumer and Serber (for a detailed discussion of the construction and properties of spin eigenfunctions, see ref 13).

The set of five Kotani spin functions ${}^{K}\Theta^6_{00;k}$ are formed by successive coupling of three α and three β one-electron spin functions according to the rules for addition of angular momenta. Each of these spin functions is fully defined by the series of partial resultant spins obtained after combining the first 1, 2, . . . , 5 one-electron spin functions, which can be used as a compact notation for the spin function:

$$\begin{aligned}
{}^{K}\Theta^6_{00;1} &\equiv \left(\tfrac{1}{2}\,1\,\tfrac{3}{2}\,1\,\tfrac{1}{2}\right)\\
{}^{K}\Theta^6_{00;2} &\equiv \left(\tfrac{1}{2}\,1\,\tfrac{1}{2}\,1\,\tfrac{1}{2}\right)\\
{}^{K}\Theta^6_{00;3} &\equiv \left(\tfrac{1}{2}\,0\,\tfrac{1}{2}\,1\,\tfrac{1}{2}\right)\\
{}^{K}\Theta^6_{00;4} &\equiv \left(\tfrac{1}{2}\,1\,\tfrac{1}{2}\,0\,\tfrac{1}{2}\right)\\
{}^{K}\Theta^6_{00;5} &\equiv \left(\tfrac{1}{2}\,0\,\tfrac{1}{2}\,0\,\tfrac{1}{2}\right)
\end{aligned} \tag{3}$$

The Kotani spin basis is orthonormal, and the weights of the components of Θ^6_{00} (see eq 2), when expressed in this basis, are given simply by the squares of the expansion coefficients $({}^{K}C_{0k})^2$ (assuming that Θ^6_{00} is normalized to unity).

Each of the five Rumer spin eigenfunctions ${}^{R}\Theta^6_{00;k}$ represents a product of three singlet two-electron spin functions:

$$\begin{aligned}
{}^{R}\Theta^6_{00;1} &\equiv (1-2,\,3-4,\,5-6)\\
{}^{R}\Theta^6_{00;2} &\equiv (1-4,\,2-3,\,5-6)\\
{}^{R}\Theta^6_{00;3} &\equiv (1-2,\,3-6,\,4-5)\\
{}^{R}\Theta^6_{00;4} &\equiv (1-6,\,2-3,\,4-5)\\
{}^{R}\Theta^6_{00;5} &\equiv (1-6,\,2-5,\,3-4)
\end{aligned} \tag{4}$$

The pairs of numbers within the brackets indicate the numbers of the electrons engaged in the singlet two-electron spin functions, e.g.,

$${}^{R}\Theta^6_{00;1} \equiv (1-2,\,3-4,\,5-6) = 2^{-3/2}[\alpha(1)\beta(2)-\alpha(2)\beta(1)]\times [\alpha(3)\beta(4)-\alpha(4)\beta(3)][\alpha(5)\beta(6)-\alpha(6)\beta(5)] \tag{5}$$

The Rumer spin functions can be visualized by means of Rumer diagrams, which bear close resemblance to the resonance structures that can be found in older organic chemistry textbooks. In fact, there is a one-to-one correspondence between ${}^{R}\Theta^6_{00;1}$– ${}^{R}\Theta^6_{00;5}$ and the five well-known resonance structures for benzene: ${}^{R}\Theta^6_{00;1}$ and ${}^{R}\Theta^6_{00;4}$ match the two Kekulé structures, while the three Dewar (or para-bonded) structures are related to ${}^{R}\Theta^6_{00;2}$, ${}^{R}\Theta^6_{00;3}$ and ${}^{R}\Theta^6_{00;5}$. In many cases, the analogy between Rumer diagrams and resonance structures allows a straightforward interpretation of the results of SC calculations in classical VB terms. The Rumer spin basis is nonorthogonal, and the weights of the individual spin functions making up Θ^6_{00} (see eq 2) have to be calculated through a more complicated expression. Two frequently used formulas have been suggested by Chirgwin and Coulson[14] and Gallup and Norbeck.[15] A disadvantage of the more popular Chirgwin-Coulson expression is that it does not guarantee that all weights will be nonnegative and smaller than unity. When Θ^6_{00} is strongly dominated by a single Rumer spin function, the weight of this spin function can exceed one, while to compensate for this, some of the other weights will have to be small negative numbers.

The Serber spin functions ${}^{S}\Theta^6_{00;k}$ are assembled similarly to the Kotani spin functions but from different building blocks, which consist of all two-electron singlet and triplet wave functions (and, in the odd-electron case, the one-electron spin function for the last electron). The Serber spin basis is orthonormal, just as the Kotani spin basis. It is very useful when analyzing the electronic structure of antiaromatic systems such as square cyclobutadiene[16] and diradicals, e.g., benzyne.[17]

The interconversion and analysis of active space spin functions (such as Θ^6_{00} in eq 2) expressed in the Rumer, Kotani and Serber spin bases can be performed in a straightforward manner with the use of a specialized code for the symbolic generation and transformation of spin eigenfunctions (SPINS, see ref 18).

As we show in the next section, during the course of the 1,3-dipolar cycloaddition of diazomethane to ethene Θ^6_{00} is dominated by a single "perfect-pairing" spin function in which the spins of the active orbitals are coupled to singlet pairs, just as in the case of the analogous reaction between fulminic acid and ethyne.[4] The Kotani, Rumer and Serber spin bases

(11) Karadakov, P. B.; Gerratt, J.; Cooper, D. L.; Raimondi, M. *J. Chem. Phys.* **1992**, *97*, 7637.
(12) Schmidt, M. W.; Baldridge, K. K.; Boatz, J. A.; Elbert, S. T.; Gordon, M. S.; Jensen, J. H.; Koseki, S.; Matsunaga, N.; Nguyen, K. A.; Su, S. J.; Windus, T. L.; Dupuis, M.; Montgomery, J. A. *J. Comput. Chem.* **1993**, *14*, 1347.
(13) Pauncz, R. *Spin Eigenfunctions*; Plenum Press: New York, 1979.
(14) Chirgwin, B. H.; Coulson, C. A. *Proc. R. Soc. London, Ser. A* **1950**, *201*, 196.
(15) Gallup, G. A.; Norbeck, J. M. *Chem. Phys. Lett.* **1973**, *21*, 495.
(16) Wright, S. C.; Cooper, D. L.; Gerratt, J.; Raimondi, M. *J. Phys. Chem.* **1992**, *96*, 7943.
(17) Karadakov, P. B.; Gerratt, J.; Raos, G.; Cooper, D. L.; Raimondi, M. *Isr. J. Chem.* **1993**, *33*, 253.
(18) Karadakov, P. B.; Gerratt, J.; Cooper, D. L.; Raimondi, M. *Theor. Chim. Acta* **1995**, *90*, 51.

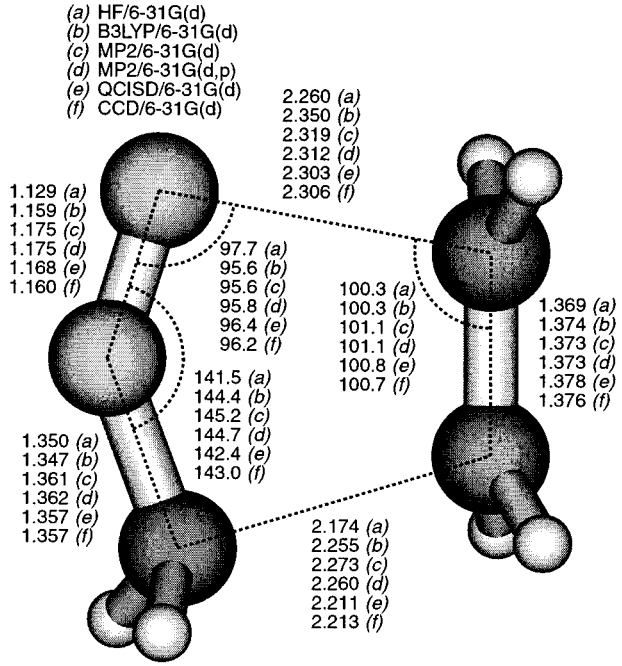

Figure 1. Geometry of the TS for the gas-phase 1,3-dipolar cycloaddition of diamethane to ethene at the (*a*) HF/6-31G(d), (*b*) B3LYP/6-31G(d), (*c*) MP2/6-31G(d), (*d*) MP2/6-31G(d,p), (*e*) QCISD/6-31G(d) and (*f*) CCD/6-31G(d) levels of theory. Bond lengths in Å, angles in degrees.

share a common spin eigenfunction of this type (${}^{K}\Theta^{6}_{00;5} = {}^{R}\Theta^{6}_{00;1} = {}^{S}\Theta^{6}_{00;5}$, see eq 5), and so there is little to be gained by reanalyzing the form of Θ^{6}_{00} within each basis. All spin-coupling coefficients reported in the next section are expressed in the Kotani spin basis, which is the "native" basis of the code used to perform the SC calculations in the present work.

Results and Discussion

The main features of the concerted C_s-symmetry geometries for the gas-phase 1,3-dipolar cycloaddition of diazomethane to ethene optimized using HF/6-31G(d), B3LYP/6-31G(d), MP2/6-31G(d), MP2/6-31G(d,p), QCISD/6-31G(d) and CCD/6-31G(d) wave functions are summarized in Figure 1. The HF/6-31G(d), B3LYP/6-31G(d) and MP2/6-31G(d) geometries shown in this figure are practically identical to those reported by Rastelli et al.[8] The differences between the TS structural parameters obtained at the MP2/6-31G(d) and MP2/6-31G(d,p) levels of theory are reasonably small (the largest difference of 0.013 Å is observed for the forming C−C bond), which suggests that the smaller 6-31G(d) basis represents an appropriate choice for post-HF descriptions of the TS and the associated reaction pathway. While the geometries optimized within the 6-31G(d) basis at the two highest levels of theory, QCISD and CCD, are very similar (the corresponding interatomic distances differ by no more than 0.003 Å, with the exception of the N−N bond length which exhibits a slightly larger variation of 0.008 Å), they stand apart from the other 6-31G(d) post-HF geometries (B3LYP and MP2) as far as the forming bond lengths are concerned. The largest difference (0.062 Å) is observed between the MP2/6-31G(d) and QCISD/6-31G(d) estimates of the length of the forming C−C bond. This suggests that the proper description of the TS geometries for 1,3-dipolar cycloadditions requires the use of well-correlated wave functions.

An attempt was also made to optimize the TS at the MP4(SDQ)/6-31G(d) level of theory, starting from the MP2/6-31G(d) geometry and using analytic MP2/6-31G(d) force constants at the first point (GAUSSIAN98 does not provide analytic Hessians for MP4 wave functions). Under these conditions, the Berny optimization procedure converged to a second-order saddle point, which was verified through diagonalization of the numerical MP4(SDQ) Hessian calculated at the final geometry.

One unexpected detail related to the MP2-level geometry optimization of diazomethane is that the lowest-energy structure turned out to be of C_s symmetry, while the optimized C_{2v} structure was shown to correspond to a first-order saddle point. This was confirmed by calculations utilizing MP2/6-31(d), MP2/6-31(d,p) and MP2/6-311++G(2d,2p) wave functions which produced values of 178.0°, 177.9° and 178.7° for the C−N−N valence angle, and 164.7°, 163.4° and 169.9° for the H−C−N−H dihedral angle (involving the central N). Geometry optimizations within all other approaches produced structures of the expected C_{2v} symmetry.

Although the C_s-symmetry TS for the gas-phase 1,3-dipolar cycloaddition of diazomethane to ethene has a plane of symmetry coincident with the heavy atoms, this plane is not present in the product of the reaction, 1-pyrazoline. The symmetry group of 1-pyrazoline is also C_s, but the plane of symmetry is coincident with the central methylene group and passes through the middle of the N=N double bond. At the CCD/6-31G(d) level of theory, the puckering angle between the C−N−N−C and C−C−C planes is equal to 159.8°. The symmetry change happens very "late", beyond 5.72 amu$^{1/2}$bohr along the IRC branch starting at the TS and leading to the product.

The electronic activation energies, activation barriers including zero-point energy corrections and standard enthalpies, entropies and Gibbs free energies of activation for the gas-phase 1,3-dipolar cycloaddition of diazomethane to ethene and for the reverse of this reaction, the gas-phase cycloelimination of ethene from 1-pyrazoline, are given in Tables 1 and 2.

The $\Delta^{\ddagger}E_{\text{elec}}$ and $\Delta^{\ddagger}(E_{\text{elec}} + \text{ZPE})$ values in Table 1 obtained at the HF/6-31G(d), B3LYP/6-31G(d) and MP2/6-31G(d) levels of theory are in excellent agreement with the results of Rastelli et al.[8] The same is true of the $\Delta^{\ddagger}H°$ values based on HF/6-31G(d) and MP2/6-31G(d) calculations, but our B3LYP/6-31G(d) estimate of the standard activation enthalpy is 0.6 kcal mol^{-1} lower than the value that can be calculated using the numbers reported in ref 8. Additionally, larger discrepancies are observed in the case of the HF/6-31G(d), B3LYP/6-31G(d) and MP2/6-31G(d) standard entropies and Gibbs free energies of activation: The corresponding $\Delta^{\ddagger}S°$ and $\Delta^{\ddagger}G°$ values from ref 8 are −29.92, −29.06, −30.96 cal mol^{-1}K^{-1}, and 42.98, 24.56, 16.73 kcal mol^{-1}, respectively. We have checked the results of our calculations very thoroughly, and it appears that the most probable explanation for the observed discrepancies is that some of the numbers reported in ref 8 may be incorrect.

According to the theoretical results of Rastelli et al.,[8] the solvent effects on the Gibbs free energy of activation for the 1,3-dipolar addition of diazomethane to ethene are small (not exceeding −1.41 kcal mol^{-1}), which suggests that the experimental gas-phase $\Delta^{\ddagger}G°$ should not be very different from the corresponding value in solution, 22.0 kcal mol^{-1} (measured in dimethylformamide at 298K).[19,20] The only theoretical estimate for $\Delta^{\ddagger}G°$ in

Table 1. Electronic Activation Energies ($\Delta^{\ddagger}E_{elec}$), Activation Barriers Including Zero-Point Energy Corrections [$\Delta^{\ddagger}(E_{elec} + ZPE)$] and Standard (taken as 298.15 K, 1 atm) Enthalpies ($\Delta^{\ddagger}H^{\circ}$), Entropies ($\Delta^{\ddagger}S^{\circ}$) and Gibbs Free Energies of Activation ($\Delta^{\ddagger}G^{\circ}$) for the Gas-Phase 1,3-Dipolar Cycloaddition of Diazomethane to Ethene[a]

method	$\Delta^{\ddagger}E_{elec}$	$\Delta^{\ddagger}(E_{elec} + ZPE)$	$\Delta^{\ddagger}H^{\circ}$	$\Delta^{\ddagger}S^{\circ}$	$\Delta^{\ddagger}G^{\circ}$
HF/6-31G(d)	32.21	34.92	33.46	−38.27	44.87
B3LYP/6-31G(d)	14.26	16.63	15.30	−37.42	26.46
MP2/6-31G(d)	5.74	8.49	6.90	−40.69	19.03
MP2/6-31G(d,p)	5.54	8.24	6.65	−40.61	18.76
QCISD/6-31G(d)	17.98	20.78	19.33	−38.17	30.71
CCD/6-31G(d)	16.31	19.13	17.66	−38.36	29.10
CCD/6-311++G(2d,2p)[b]	16.94	19.76	18.29	−38.36	29.73
MP4(SDTQ)/6-311++G(2d,2p)[b]	10.04	12.87	11.39	−38.36	22.83
CCSD(T)/6-311++G(2d,2p)[b]	13.53	16.35	14.88	−38.36	26.32

[a] All energetical quantities are in kcal mol^{-1}, entropies are in cal mol^{-1} K^{-1}. [b] Single-point CCD/6-311++G(2d,2p)//CCD/6-31G(d), MP4(SDTQ)/6-311++G(2d,2p)//CCD/6-31G(d) and CCSD(T)/6-311++G(2d,2p)//CCD/6-31G(d) energies combined with CCD/6-31G(d) zero-point energy corrections, standard entropies and thermal corrections to standard enthalpies and Gibbs free energies.

Table 2. $\Delta^{\ddagger}E_{elec}$, $\Delta^{\ddagger}(E_{elec} + ZPE)$, $\Delta^{\ddagger}H^{\circ}$, $\Delta^{\ddagger}S^{\circ}$ and $\Delta^{\ddagger}G^{\circ}$ Values for the Gas-Phase Cycloelimination of Ethene from 1-Pyrazoline[a]

method	$\Delta^{\ddagger}E_{elec}$	$\Delta^{\ddagger}(E_{elec} + ZPE)$	$\Delta^{\ddagger}H^{\circ}$	$\Delta^{\ddagger}S^{\circ}$	$\Delta^{\ddagger}G^{\circ}$
HF/6-31G(d)	74.84	70.15	70.60	2.09	69.98
B3LYP/6-31G(d)	51.31	47.26	47.85	2.77	47.02
MP2/6-31G(d)	48.49	44.38	45.00	3.91	43.84
MP2/6-31G(d,p)	47.66	43.65	44.26	3.84	43.12
QCISD/6-31G(d)	60.51	56.13	56.74	3.64	55.65
CCD/6-31G(d)	61.45	57.23	57.81	3.50	56.77
CCD/6-311++G(2d,2p)	56.41	52.19	52.78	3.50	51.73
MP4(SDTQ)/6-311++G(2d,2p)	46.01	41.79	42.38	3.50	41.32
CCSD(T)/6-311++G(2d,2p)	50.63	46.41	47.00	3.50	45.95

[a] Further details as in Table 1, including footnote related to CCD/6-311++G(2d,2p), MP4(SDTQ)/6-311++G(2d,2p) and CCSD(T)/6-311++G(2d,2p) results.

Table 1 that comes very close to this experimental value is the one obtained at the MP4(SDTQ)/6-311++G(2d,2p)//CCD/6-31G(d) level of theory. This confirms an earlier observation[8] that the best agreement between the theoretical and experimental $\Delta^{\ddagger}G^{\circ}$ values is achieved if the electronic activation energy is calculated using MP4(SDTQ) wave functions. However, most quantum chemists would be inclined to consider CCSD(T) a more accurate approach than MP4(SDTQ) (see, e.g., ref 21); the CCSD(T)/6-311++G(2d,2p)//CCD/6-31G(d) Gibbs free energy of activation is 3.49 kcal mol^{-1} higher than its MP4(SDTQ)/6-311++G(2d,2p)//CCD/6-31G(d) counterpart. It seems unlikely that extension of the basis set beyond 6-311++G(2d,2p) would bring the CCSD(T) estimate of $\Delta^{\ddagger}G^{\circ}$ much closer to the experimental value. In fact, in view of the CCD/6-31G(d) and CCD/6-311++G(2d,2p)//CCD/6-31G(d) results in Table 1, the CCSD(T) estimate could even be expected to increase slightly upon further basis set extension. In the absence of an experimental gas-phase $\Delta^{\ddagger}G^{\circ}$ value, and given the fact that Rastelli et al.[8] used cyclohexane and water and not dimethylformamide in their solvent effect calculations, it is very difficult to decide if the CCSD(T)/6-311++G(2d,2p)//CCD/6-31G(d) gas-phase $\Delta^{\ddagger}G^{\circ}$ value is more or less reliable than its MP4(SDTQ)/6-311++G(2d,2p)//CCD/6-31G(d) counterpart. Having said that, it is interesting to observe that the oscillating HF/6-311++G(2d,2p)//CCD/6-31G(d), MP2/6-311++G(2d,2p)//CCD/6-31G(d), MP3/6-311++G(2d,2p)//CCD/6-31G(d) and MP4(SDTQ)/6-311++G(2d,2p)//CCD/6-31G(d) values for the electronic activation energy $\Delta^{\ddagger}E_{elec}$: 35.70, 5.09, 16.31 and 10.04 kcal mol^{-1}, respectively, can be expected to converge to a limit which would not be too far off the CCSD(T)/6-311++G(2d,2p)//CCD/6-31G(d) electronic activation energy of 13.53 kcal mol^{-1} (see Table 1). A similar observation can be made for the analogous series of HF, MP2, MP3 and MP4 $\Delta^{\ddagger}E_{elec}$ values for the gas-phase cycloelimination of ethene from 1-pyrazoline which runs as 73.00, 41.96, 56.54 and 46.01 kcal mol^{-1}, and is likely to converge to a limit close to the CCSD(T) value of 50.63 kcal mol^{-1} (see Table 2).

The most important features of the SC(6)/6-31G wave function (1) calculated at three points from the MP2/6-31G(d) IRC for the gas-phase 1,3-dipolar cycloaddition of diazomethane to ethene are summarized in Figure 2 and Tables 3−5. One of the IRC points coincides with the MP2/6-31G(d) TS, and the other two correspond to "before"-TS (R_{IRC} = 1.18901 amu$^{1/2}$bohr) and "after"-TS (R_{IRC} = − 1.19702 amu$^{1/2}$bohr) geometries, which are sufficiently well-separated from the TS to make the changes in the electronic structure of the reacting system, as depicted by the SC wave function, easy to observe. At all three points the SC(6)/6-31G wave function recovers a sizable proportion (not less than 94.2%) of the correlation energy associated with its "6-in-6" complete-active-space self-consistent field [CASSCF(6,6)/6-31G] counterpart (see Table 3).

It is interesting to mention that the calculation of the CASSCF(6,6)/6-31G wave functions at the three points along the IRC required different initial guesses for the active-space orbitals. In all three cases, the doubly occupied orbitals were initially chosen as the canonical HF/6-31G orbitals with numbers 12, 18 and 19, but the corresponding selected virtuals had to be numbers 21, 22 and 34 at R_{IRC} = 1.18901 amu$^{1/2}$bohr; 20, 22 and 34

(19) Sustmann, R.; Wenning, E.; Huisgen, R. *Tetrahedron Lett.* **1977**, *10*, 877.
(20) Geittner, J.; Huisgen, R.; Sustmann, R. *Tetrahedron Lett.* **1977**, *10*, 881.
(21) Jensen, F. *Introduction to Computational Chemistry*; Wiley: Chichester, 1999; p 145.

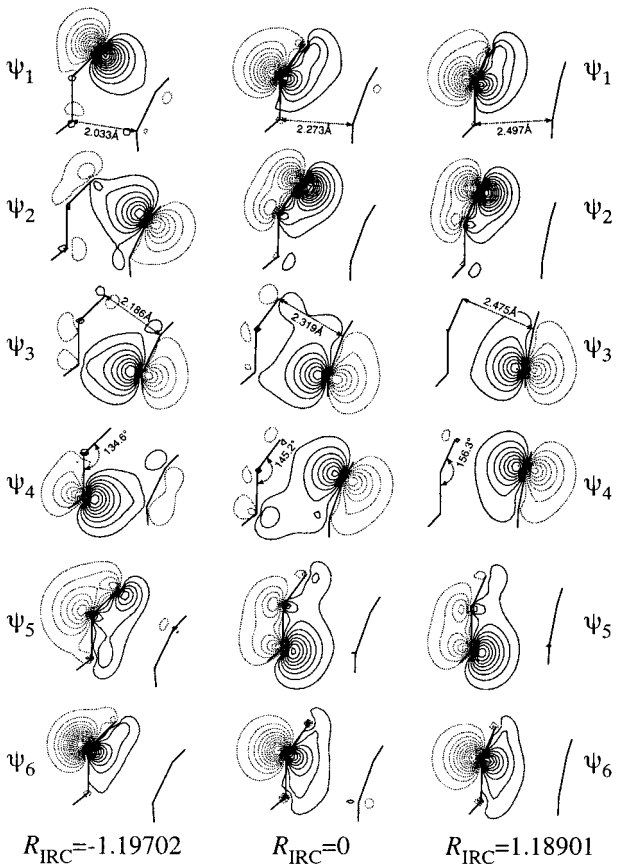

Figure 2. Active (valence) orbitals ψ_1, ψ_2, . . . , ψ_6 from the SC wave function for the gas-phase 1,3-dipolar cycloaddition of diazomethane to ethene at "after"-TS, TS and "before"-TS geometries ($R_{IRC} = -1.19702$, 0, 1.18901 amu$^{1/2}$bohr). Contour plots of the orbitals in the plane of the heavy atoms with separation of 0.05 between the levels produced by MOLDEN.[23] Dotted lines correspond to negative values.

Table 3. HF, SC(6) and CASSCF(6,6) Total Energies Correlation Energies for the 1,3-Dipolar Cycloaddition of Diazomethane to Ethene Evaluated within the 6-31G Basis at Different Points along the MP2/6-31G(d) IRC[a]

quantity	$R_{IRC} = -1.19702$	TS ($R_{IRC} = 0$)	$R_{IRC} = 1.18901$
E(HF)	−225.72318	−225.71520	−225.72722
E(SC)	−225.80268	−225.79679	−225.81066
E(CASSCF)	−225.80705	−225.80178	−225.81349
ΔE^{corr}(SC)	−0.07950 (94.8%)	−0.08159 (94.2%)	−0.08344 (96.7%)
ΔE^{corr}(CASSCF)	−0.08387	−0.08658	−0.08627

[a] All energies in hartree and "distances" along the IRC in amu$^{1/2}$bohr

at the TS; and 20, 23 and 34 at $R_{IRC} = -1.19702$ amu$^{1/2}$bohr. This highlights an eventual complication related to the use of standard CASSCF wave functions in IRC calculations. Unless the step size is chosen to be sufficiently small, it may prove difficult to maintain a consistent active space along the reaction path. This is one of the reasons behind our decision to switch to an IRC calculated with MP2 rather than to use a CASSCF-level IRC (as in our description of the reaction mechanism of the gas-phase 1,3-dipolar addition of fulminic acid to ethyne[4]). The second reason follows from the recognition of the importance of dynamic electron correlation effects for the correct description of TS geometries and activation barriers (see, e.g., ref 22), which was also highlighted earlier in this section by the discussion of differences between TS geometries calculated at different levels of theory.

The analysis of the changes in the SC wave function throughout the gas-phase 1,3-dipolar cycloaddition of CH_2N_2 to C_2H_4 (see below) indicates that the reacting system retains significant closed-shell character along the whole span of the reaction coordinate connecting reactants, TS and product. As a consequence, in this particular case and possibly for other 1,3-dipolar additions, the use of wave functions that utilize a closed-shell HF reference such as the MPn, QCISD and CC constructions is sufficiently well-justified. The evolutionary, rather than revolutionary, character of the modifications of the qualitative features of the SC wave function along the reaction pathway (see below) suggests that the qualitative side of the SC description of the reaction mechanism should not be overly sensitive to the accuracy of the IRC. In fact, the forming C−C and C−N bond lengths at the CCD/6-31G(d) and QCISD/6-31G(d) TS geometries are very close to those observed at an IRC point just after the TS along the TS to product branch of the MP2/6-31G(d) IRC. As a consequence, the SC calculations at the CCD/6-31G(d) and QCISD/6-31G(d) TS geometries would only indicate a slightly more advanced stage of formation of the new bonds as compared to the MP2/6-31G(d) TS geometry but would not provide new qualitative elements that are not present in the current analysis. However, if a more accurate, say, QCISD- or CCD-level, IRC is required in other applications, it could be calculated by GAUSSIAN98[10] using numerical differentiation with a small step size to obtain the Hessian at the TS.

The six SC orbitals from the rightmost column in Figure 2 fall into two distinct groups, each of which is associated with one of the two reactants. The ethene carbon−carbon π bond is the obvious source for two of the orbitals, ψ_3 and ψ_4. The remaining four orbitals are localized on the diazomethane fragment, and it is not difficult to recognize that they are closely related to the well-known SC description of isolated CH_2N_2[6,24] according to which the central nitrogen atom is "hypercoordinate", taking part in more than four covalent bonds: an almost double bond to C and an almost triple bond to the terminal N. In an undistorted C_{2v}-symmetry diazomethane molecule, orbitals ψ_5 and ψ_6 would be responsible for the π component of the carbon−nitrogen bond, while orbitals ψ_1 and ψ_2 would describe one of the π components (the one that points out of the molecular plane) of the nitrogen−nitrogen multiple bond. This orbital classification is fully supported by the values of the orbital overlaps at $R_{IRC} = 1.18901$ amu$^{1/2}$bohr (see Table 4). The largest overlap integrals, with one exception, are between orbitals that reside on one and the same fragment and form bonds of almost π-character, i.e., $\langle\psi_1|\psi_2\rangle$, $\langle\psi_3|\psi_4\rangle$ and $\langle\psi_5|\psi_6\rangle$. The exception is provided by the overlap between orbitals ψ_1 and ψ_6, which are both localized mostly about the central N but participate in different bonds. As demonstrated by the numbers in the last column of Table 5, at $R_{IRC} = 1.18901$ amu$^{1/2}$bohr the active-space spin-coupling pattern Θ^6_{00} (see eq 2) is

(22) Borden, W. T.; Davidson, E. R. *Acc. Chem. Res.* **1996**, *29*, 67.
(23) Schaftenaar, G. *MOLDEN (A Pre- and Postprocessing Program of Molecular and Electronic Structure)*; CAOS/CAMM Center: University of Nijmegen, The Netherlands.
(24) Cooper, D. L.; Gerratt, J.; Raimondi, M.; Wright, S. C. *Chem. Phys. Lett.* **1987**, *138*, 296.

Table 4. Overlap Integrals between the SC Orbitals at R_{IRC} = 1.18901 amu$^{1/2}$bohr (top values), at the TS (middle values), and at R_{IRC} = −1.19702 amu$^{1/2}$bohr (bottom values)

	ψ_1	ψ_2	ψ_3	ψ_4	ψ_5	ψ_6
		0.762	0.150	0.217	0.442	0.926
ψ_1	1	0.762	0.240	0.300	0.508	0.925
		0.552	0.078	0.038	0.525	0.346
			0.189	0.219	0.417	0.593
ψ_2		1	0.303	0.303	0.473	0.596
			0.288	0.107	0.122	0.218
				0.648	0.307	0.220
ψ_3			1	0.710	0.457	0.335
				0.702	0.110	0.168
					0.207	0.159
ψ_4				1	0.452	0.282
					0.294	0.193
						0.646
ψ_5					1	0.690
						0.848
ψ_6						1

Table 5. Weights $(C_{0k})^2$ of the Kotani Spin Functions Included in Θ^6_{00} (see eq 2) at Different Points along the MP2/6-31G(d) IRC for the 1,3-Dipolar Cycloaddition of Diazomethane to Ethene

k	Spin function	R_{IRC} = −1.19702	TS (R_{IRC} = 0)	R_{IRC} = 1.18901
1	$(\frac{1}{2}1\frac{3}{2}1\frac{1}{2})$	0.00071	0.04993	0.05061
2	$(\frac{1}{2}1\frac{1}{2}1\frac{1}{2})$	0.00128	0.01233	0.01809
3	$(\frac{1}{2}0\frac{1}{2}1\frac{1}{2})$	0.00249	0.05975	0.00648
4	$(\frac{1}{2}1\frac{1}{2}0\frac{1}{2})$	0.07795	0.00454	0.00091
5	$(\frac{1}{2}0\frac{1}{2}0\frac{1}{2})$	0.91757	0.87346	0.92392

decidedly dominated by its perfect-pairing component $\Theta^6_{00;5} \equiv (^1/_2 0^1/_2 0^1/_2)$, in which the spins of the strongly overlapping orbitals ψ_1 and ψ_2, ψ_3 and ψ_4, and ψ_5 and ψ_6 are coupled to singlet pairs.

The comparison between the shapes of the SC orbitals from the rightmost and middle columns in Figure 2 shows that the most pronounced changes on the way from separated reactants to TS are displayed by ψ_3 and ψ_4. Upon further progress of the reaction these orbitals become involved in the forming carbon−carbon bond (see the leftmost column in Figure 2). The distance between the carbons to be joined by this bond is shorter than that between the carbon and nitrogen atoms from the other forming bond at all three IRC points in Figure 2 and, as a consequence, the major changes in the shapes of the orbitals involved in that other bond, ψ_1 and ψ_2, occur after the TS. It is interesting to contrast the observed "earlier" formation of the carbon−carbon bond with the fact that in the final product of the reaction, 1-pyrazoline, this bond is longer than its carbon−nitrogen counterpart [1.531 Å against 1.493 Å at the CCD/6-31G(d) level of theory]. We have not analyzed the evolution of the two forming bonds at geometries close to that of 1-pyrazoline. At such geometries the six active orbitals in the SC(6) wave function are sufficient to accommodate just one of the two carbon−carbon bonds, one of the two carbon−nitrogen bonds and one of the nitrogen lone pairs. However, the two carbon−carbon and carbon−nitrogen bonds, as well as both nitrogen lone pairs become symmetry-equivalent in the product which implies that its proper description would require a SC wave function with at least 12 active orbitals.

Just as in the case of the 1,3-dipolar cycloaddition between fulminic acid and ethyne,[4] here once again we observe SC orbitals which shift between the two reacting molecules during the course of the reaction. Initially orbital ψ_4 is associated with one of the ethene carbons, at the TS it becomes a three-center orbital, and by the end of the reaction it is already mostly localized on the diazomethane carbon and gets involved, together with ψ_3, in the new carbon−carbon bond. Another orbital, ψ_2, relocates from the terminal nitrogen in diazomethane to the incoming ethene carbon and also temporarily attains three-center character in the process. Some of this character is still noticeable in its contour plot at R_{IRC} = −1.19702 amu$^{1/2}$bohr) where ψ_2 forms the new carbon−nitrogen bond through interaction with ψ_1.

The changes in the shapes of the remaining two orbitals, ψ_5 and ψ_6, are relatively minor and suggest that at the TS these orbitals still realize a partial π bond between the carbon and central nitrogen atoms of the CH_2N_2 moiety. After the TS, both orbitals shift in the direction of the nitrogens to form the lone pair on the central nitrogen (see the leftmost column in Figure 2). The tails toward the terminal N that are observed in both orbitals at R_{IRC} = − 1.19702 amu$^{1/2}$bohr are most probably a consequence of the already mentioned inequivalent representation of the two in-plane N lone pairs within the SC(6) wave function. The second pair, on the terminal N, is described by a doubly occupied core orbital in the present work.

Compared to the profound reshaping of the SC orbitals throughout the course of the reaction, the parallel changes in the values of the orbital overlaps (see Table 4) and in the composition of the active space spin-coupling pattern (see Table 5) appear to be rather mundane. At the TS, in continuation of the trend started at R_{IRC} = 1.18901 amu$^{1/2}$bohr, the largest overlap integrals remain $\langle\psi_1|\psi_2\rangle$, $\langle\psi_3|\psi_4\rangle$, $\langle\psi_5|\psi_6\rangle$ and $\langle\psi_1|\psi_6\rangle$. The higher degree of delocalization of the SC orbitals is reflected in moderate increases in the magnitudes of all other overlaps. After the TS, at R_{IRC} = −1.19702 amu$^{1/2}$bohr, the largest overlap integrals are once again $\langle\psi_1|\psi_2\rangle$, $\langle\psi_3|\psi_4\rangle$ and $\langle\psi_5|\psi_6\rangle$. The magnitudes of almost all other overlaps, including $\langle\psi_1|\psi_6\rangle$, are reduced as a consequence of the more localized nature of the orbitals. The relatively large overlap $\langle\psi_1|\psi_5\rangle$ should decrease further along the IRC, in parallel with the expected increase of $\langle\psi_1|\psi_2\rangle$ as the formation of the new nitrogen−carbon bond approaches completion.

Just as before the TS, the perfect-pairing spin eigenfunction $\Theta^6_{00;5} \equiv (^1/_2 0^1/_2 0^1/_2)$ continues to dominate the active-space spin-coupling pattern (see Table 5) at and after the TS. Its slightly lower weight at the TS is related to the increased overlaps between the SC orbitals, which create better opportunities for "resonance". However, the extent of this "resonance" is insufficient to promote speculation that the TS could have other than nonaromatic character.

Taken together, the analysis of the changes in the shapes of the SC orbitals, in the overlaps between these orbitals and in the composition of the active-space spin-coupling pattern clearly indicate that the orbital pairs (ψ_1, ψ_2), (ψ_3, ψ_4) and (ψ_5, ψ_6) are retained throughout the course of the gas-phase 1,3-dipolar cycloaddition of

diazomethane to ethene. The orbital pair shifts responsible for the bonding rearrangements associated with this reaction can be summarized through scheme B (the hollow dots show the second N lone pair which is held within the core space).

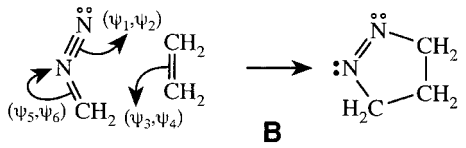

B

Apart from some relatively minor differences in the "timelines" of changes in the shapes of some of the orbitals along the reaction path, this mechanism is very similar to that of the gas-phase 1,3-dipolar cycloaddition between fulminic acid and ethyne (see scheme A in the Introduction and ref 4). The minor differences follow from the fact that, as was mentioned in the Introduction, the π N−O bond in fulminic acid is strongly polarized toward the oxygen atom, while the N−N π bond in diazomethane is much more evenly shared by the central and terminal nitrogens. As a result, the orbital pair responsible for the N−N π bond in diazomethane is less mobile and shifts over to form one of the bonds closing the 1-pyrazoline ring well after the TS, in contrast to the case of the reaction between fulminic acid and ethyne, in which the corresponding orbital pair shift is already in an advanced stage at the TS.

Conclusions

The SC model for the electronic mechanism of the gas-phase 1,3-dipolar cycloaddition of diazomethane to ethene presented in this work provides a second example of a reaction in which the bonding rearrangements follow a heterolytic pattern, characterized by the movement of well-identifiable orbital pairs that are retained along the entire reaction path from reactants to product. When we first encountered an electronic mechanism of this type in the SC study of the gas-phase 1,3-dipolar cycloaddition between fulminic acid and ethyne,[4] we were surprised to observe that a VB-style wave function, such as the one used in SC theory, would allow certain active orbitals to detach themselves completely, during the course of the reaction, from the atomic centers with which they were associated in the reactants and end up localized about different atomic centers in the product. The current work reconfirms that the SC wave function has the flexibility required to describe both homolytic and heterolytic reaction mechanisms within an ansatz that utilizes just a single orbital product, the changes in which can be associated with the half- and full-arrow reaction schemes from standard organic chemistry textbooks.

Our results for two gas-phase 1,3-dipolar cycloadditions, between diazomethane and ethene and between fulminic acid and ethyne,[4] suggest that it is most likely that the majority of concerted 1,3-dipolar cycloaddition reactions follow an electronic mechanism of a heterolytic type which can be expressed simply in a fashion analogous to schemes A and B. One consequence is that it seems somewhat unlikely to encounter a 1,3-dipolar cycloaddition passing through an aromatic TS. A further consequence of the present work, of a methodological character, is that in most cases it should be possible to obtain highly accurate descriptions of the most important regions of the potential surfaces corresponding to reactions of this type using wave functions based on a closed-shell reference.

JO015560A